Pharmaceutical Sciences Asia

Pharm Sci Asia 2025; 52(2), 206-215

DOI:10.29090/psa.2025.02.24.2546

Research Article

Elsholtzia ciliata leave-extract loaded silk microparticles as a prospective anti-oxidative skin cosmetic

Khanh Nguyen Di[1], Ngoc Yen Nguyen[2], Duong Ngoc Nhu Y[2], Vo Thi Kha Vi[2], Nguyen Thai Hai Khiem[2], Nguyen Trong Tuan[2], Manh Quan Nguyen[3], Duy Toan Pham[2,*]

[1] Faculty of Technology, Dong Nai Technology University, Bien Hoa City, Vietnam
[2] Department of Health Sciences, College of Natural Sciences, Can Tho University, Campus II, 3/2 Street, Can Tho 900000, Vietnam
[3] Department of Analytical Chemistry-Drug Quality Control, Faculty of Pharmacy, Can Tho University of Medicine and Pharmacy, 179 Nguyen Van Cu Street, Can Tho 900000, Vietnam

ABSTRACT

Elsholtzia ciliata leaf extract (EC) is known for its potent antioxidant properties, largely attributed to its rich polyphenol content. However, the challenge of polyphenol uncontrolled release has limited its application. This study, for the first time, introduces a potential solution, EC-loaded silk fibroin microparticles (FMP-EC), designed to be a promising anti-oxidative skin cosmetic with controlled polyphenol release. Firstly, by varying the extraction conditions, the optimal condition was EtOH 70% as solvent, powder: solvent ratio of 1:40 w/v, temperature of 50°C, extraction time of 30 min, and with ultrasound, which yielded EC with 93.45 mg GAE/g DPW. The EC was then incorporated into the FMP by the simple one-pot desolvation method, which possessed a polyphenol loading efficiency of ~30%. The particle sizes of FMP-EC could be controlled by adjusting the EC initial loading content. The FMP-EC were analyzed using FT-IR spectroscopy, which showed interactions between particles compositions; and scanning electron microscopy, which demonstrated round-shape particles with smooth surfaces. Interestingly, in simulated skin pH, the FMP-EC polyphenol release was dependent on the EC loading content, with gradual release profiles of 60-74% for 6 h, following the Korsmeyer-Peppas model, suggesting that the release process involved diffusion mixed with fibroin degradation. Antioxidant DPPH assay denoted the IC_{50} values of FMP-EC was moderate (~160-190 µg/mL, depending on the formulas). Conclusively, the novel FMP-EC formulation offers a controlled and sustained release of polyphenols in EC, which could be further researched to become a potential skin cosmetic.

Keywords:
Elsholtzia ciliata; antioxidant; fibroin; microparticles; polyphenol

1. INTRODUCTION

Aging is one of the hidden risks that human faces, as it impacts both beauty and health[1]. The most noticeable symptom of aging is the skin, which is the human biggest organ, in terms of size and volume[2]. The skin is mostly impacted by the environment, since it is constantly exposed to UV radiation from the sun, dust, and pollution, making skin conditions the fourth major source of non-fatal disease burden in human[3]. Thus, skin care is becoming increasingly important, particularly in the cosmetics industry. Oxidation is a major problem for cosmetic products in the battle against skin aging[4]. To this end, anti-oxidative agents such as plant polyphenols are the outstanding solutions for skin aging[5,6].

***Corresponding author:**
* Duy Toan Pham Email: pdtoan@ctu.edu.vn

Polyphenols are secondary chemicals found in plants, with over 10,000 structurally identified compounds[7]. They all have the structural trait of having an aromatic ring connected to one or more hydroxyl groups, which can be free, esterified, or glycosidic connections with sugars. Polyphenols are classified into four kinds based on the quantity of phenolic groups and structural components, including (1) flavonoids, (2) stilbenes, (3) lignans, and (4) phenolic acids[8]. Polyphenols can protect the body from the detrimental effects of free radicals and UV radiation, together with a variety of other biological properties, including anti-diabetic[9], anti-cancer[10], anti-inflammatory[11], cardiovascular protection[12], bone protection[13], blood pressure lowering[14], and antibacterial and antiviral properties[15].

Among numerous polyphenol-containing plants[16], *Elsholtzia ciliata* leave-extract (EC) has been proven its high antioxidant activity and can scavenge radicals such as 2,2-diphenyl-1-picrylhydrazyl (DPPH) and 2,2'-azino-bis (3-ethylbenzothiazoline)-6-sulfonic acid (ABTS), with IC_{50} values of 495.80 ± 17.16 and 73.59 ± 3.18 µg/mL, respectively[17]. Thus, EC has prospective applications in the preparation of antioxidant products. However, when being used in cosmetics, it is critical to monitor the quantity of polyphenols that release and accumulate on the skin over time, ensuring that polyphenols are progressively provided during the process of utilizing the active component. This guarantees that the skin can properly employ it while also preventing polyphenol degradation. To achieve this, a delivery system, with biocompatible, non-cytotoxic, and biodegradable materials, is necessary for the controlled release of EC polyphenols.

For that reason, silk fibroin is an appropriate carrier material, as it is recognized by The US Food and Drug Administration (FDA) as safe for human use[18]. Fibroin is a protein with a β-sheet-antiparallel structure and consists of a heavy chain and a light chain joined by P25, a glycoprotein with a 6:6:1 ratio[19]. The heavy peptide chain is made up of common amino acids such as glycine (43%), alanine (30%), and serine (12%), which forms 12 lipophilic segments joined by 11 hydrophilic segments[20,21]. Fibroin amphiphilic structure allows it to self-reform into microparticles (FMP) or nanoparticles (FNP) without a catalyst[22]. As a result, fibroin has enormous application potential in the development of active component loading systems. Furthermore, fibroin demonstrates the capacity to preserve active substances from the impacts of the pH environments and temperatures[23]. For instance, FMP or FNP have been successfully fabricated for the delivery of plant extracts of guava[23], wedelia[5], and red wine[24].

Herein, this work further explored the ability of FMP in encapsulating the EC, for the purpose of anti-oxidation in skin cosmetic. The EC extraction process was first optimized, in terms of polyphenol contents, by varying different conditions. Then, the EC was loaded into the FMP by the desolvation method, followed by physicochemical characterizations of particles sizes, shapes, interactions, and *in vitro* release profiles in simulated skin condition. Finally, the particles antioxidant action was evaluated by the DPPH assay.

2. MATERIALS AND METHODS

2.1. Materials

Elsholtzia ciliata leaves were purchased at Thanh Binh Herbal Tea Company, Go Vap, Ho Chi Minh City, Vietnam. Raw silk cocoons were acquired from Truc Ninh, Nam Dinh, Vietnam. Fibroin was extracted and purified from silk cocoons following the established protocol[21,25]. Sigma-Aldrich (Singapore) provided dialysis membranes, DPPH, Folin-Ciocalteu, and ascorbic acid. Xilong (China) supported ethanol (EtOH), sodium carbonate (Na_2CO_3), calcium chloride ($CaCl_2$), and calcium nitrate tetrahydrate ($Ca(NO_3)_2.4H_2O$).

2.2. *Elsholtzia ciliata* extraction

The fresh undamaged leaves were cleaned, dried in the shade, and pulverized into powder. The leave powder moisture was determined using a moisture drying balance (Kern Dab, Germany). The EC extraction was conducted using the standard maceration method in EtOH with the varied conditions of (1) EtOH concentrations (50%, 60%, 70%, 80%, 90%, and 99.9% v/v), (2) temperature (40°C, 45°C, 50°C, 55°C, and 60°C), (3) plant powder and EtOH ratio (1:10, 1:15, 1:20, 1:25, 1:30, 1:35, 1:40, 1:45, and 1:50 w/v), (4) extraction time (1, 2, 3, 4, and 5 h), and (5) with/without ultrasound (for 0.5, 1, 1.5, 2, and 2.5 h). The total polyphenol content was used to determine the optimal factors. The extraction efficiency (H%) was also calculated using **Equation (1)**.

$$H\% = \frac{\text{Weight of the EC extract}}{\text{Weight of the dry powder}} \times 100 \quad (1)$$

2.3. Extract polyphenols quantification

The total polyphenol content of EC was measured using UV-Vis spectroscopic method employing the Folin-Ciocalteau reagent[26]. The extracts or standard solution (0.5 mL) was combined with 2.5 mL Folin-Ciocalteau solution (10% w/v) and incubated for 5 min at room temperature, followed by the addition of 2.5 mL Na_2CO_3 solution (5% w/v). The mixture was agitated, incubated at room temperature for another 1 h, and its absorbance was UV-Vis measured at 765 nm. Gallic acid was utilized as a reference to construct the standard curve ($y = 0.1084x - 0.0005$, $R^2 = 0.9995$), and the total polyphenol content was calculated as mg gallic

equivalent in dry powder weight (mg GAE/g DPW), utilizing **Equation (2)**.

$$\text{Total polyphenol content} = \frac{\text{Polyphenol concentration (µg/mL)} \times 5.5 \times 10^3}{\text{Weight of the dry powder}} \times 100 \quad (2)$$

2.4. Preparation of silk fibroin microparticles

The blank (unloaded) FMP and EC loaded FMP (FMP-EC) were fabricated by the one-pot desolvation process[5,23]. For the blank FMP, EtOH (70% v/v) was gradually added to the fibroin aqueous solution (1% w/v) with the fibroin/EtOH ratios of 1:1, 1:2, 1:3, 1:4, 1:5, and 1:6 v/v. The mixture was agitated for 1 h and stabilized for 24 h before being centrifuged at 6,000 rpm for 10 min to obtain the FMP, which were washed multiple times with water by centrifugation. The particles were then freeze-dried for further experiments. The optimal EtOH/fibroin ratio was the one that yielded the smallest particle sizes.

The FMP-EC were manufactured in the similar approach, utilizing the optimal fibroin/EtOH ratio obtained from the blank FMP experiment. The EC ethanolic extract (3 mL) containing a total polyphenol content of 600 µg/mL (FMP-EC6) or 900 µg/mL (FMP-EC9) was slowly added to 1 mL of fibroin aqueous solution (1% w/v), agitated for 1 h, stabilized for 24 h, and centrifuged at 6,000 rpm for 10 min to obtain the FMP-EC. The supernatants, after particles washing, were combined and determined the un-encapsulated polyphenol content using the same approach described in **section 2.3**. The polyphenol loading efficiency (LE%) was calculated using **Equation (3).**

$$LE\% = \frac{Amount\ of\ total\ polyphenol\ in\ the\ particles}{The\ initial\ amount\ of\ polyphenol} \times 100 \quad (3)$$

2.5. Particles characterizations

To determine the chemical interactions, the freeze-dried particles were mixed with KBr, formed into thin pellets, and FT-IR analyzed with a NICOLET 6700 (Thermo) spectrophotometer (wavenumber range 4000-500 cm^{-1}, resolution 4.0 cm^{-1}) in a desiccated air purge. The empty KBr pellet was used to calculate background signals, which were later removed from the sample data.

The crystallization intensity of the sample was estimated using the FT-IR spectra and the crystallinity index of the amide I (CI IRI) and amide II (CI IRII) peaks of fibroin[20]. The CI IRI and CI IRII were calculated using the **Equation (4) and (5)**, with D_x is the intensity at peak x cm^{-1}.

$$CI_{IRI} = D_{1622}/(D_{1622} + D_{1646}) \quad (4)$$

$$CI_{IRII} = D_{1517}/(D_{1517} + D_{1560}) \quad (5)$$

The particle size was measured using the zeta sizer machine (SZ-100 Horiba) using dynamic light scattering method, following the manufacturer protocol.

2.6. *In vitro* release profile in simulated skin condition

The FMP-EC, with the amount equivalent to 1,000 µg/mL of polyphenol content, were put into 20 mL of phosphate buffer pH 5.5, simulating the skin pH, and uniformly disseminated at 37°C for 6 h. Regarding the skin surface temperature, the skin is a highly fluctuate organ, which is influenced by several factors, including ambient temperature, blood flow to the skin, metabolism, and physiological responses such as sweating. The skin surface temperature on the trunk typically ranges from 33.5 to 36.9°C, which made 37°C an appropriate testing temperature[27]. Every 30 min, 1 mL of the dispersion was aspirated to measure the release polyphenol content and compensated with 1 mL of fresh buffer. The withdrawn samples were centrifuged for 2 min at 12,000 rpm, and the supernatant was spectroscopic analyzed regarding its polyphenol content, following the procedure described in **section 2.3**, with the gallic acid standard curve in phosphate buffer pH 5.5 (concentration range of 2 to 10 µg/mL, maximum wavelength of 754 nm, $y = 0.1149x + 0.0087$, $R^2 = 0.9995$). The percentages of cumulative polyphenol release were calculated by **Equation (6)**.

$$\%\text{Polyphenol release} = \frac{20C_t + \sum_t^{t-1} C_i}{M_0 - \sum_t^{t-1} M_i} \text{ x } 100 \quad (6)$$

where C_t/C_i are the polyphenol contents at the time t/i, M_0/M_i are the initial polyphenol content and the withdrawal polyphenol content at time i.

To understand the release kinetics, typical models were utilized, including the zero-order model, first-order model, Korsmeyer-Peppas model, Higuchi model, and Hixson-Crowell model (**Equation (7-11)**).

$$M_t = M_0 + k_0 t \quad (7)$$

$$\ln(M_t) = \ln(M_0) - k_1 t \quad (8)$$

$$\frac{M_t}{M_0} = k_{KP} t^n \quad (9)$$

$$M_t = k_H t^{1/2} \quad (10)$$

$$M_t^{1/3} = M_0^{1/3} - k_{HC} t \quad (11)$$

where M_0/M_t are the polyphenol initial amount and polyphenol release amount at the time t; $k_0/k_1/k_{KP}/k_H/k_{HC}$ are the release constants of the

zero-order, first-order, Korsmeyer-Peppas, Higuchi, and Hixson-Crowell model, respectively.

2.7. Antioxidant activity test

The free radical scavenging activity of FMP-EC, as well as the free EC, and vitamin C as a reference, was assessed using the standard DPPH assay. For this, 500 µL DPPH solution in EtOH (0.2 mM) was mixed with either vitamin C to get a final concentration range of 0, 1.5, 3, 4.5, 6, 7.5, and 9 µg/mL, or the FMP-EC and free EC to get the final polyphenol concentration range of 0, 5, 10, 15, and 20 µg/mL. The mixtures were incubated at room temperature for 30 min in the dark, followed by spectroscopic measured at 522 nm. The blank sample contained no vitamin C nor extract. The spectral absorbance value recorded after the reaction was used to calculate the percentage of DPPH free radical inhibition using **Equation (12)**.

$$\text{DPPH scavenging effect (\%)} = \frac{\text{Blank absorbance} - \text{Sample absorbance}}{\text{Blank absorbance}} \times 100 \quad (12)$$

Standard curves were then created using the DPPH inhibition percentages obtained at various concentrations. The IC_{50} value (test sample concentration that inhibits 50% of DPPH free radicals) was then calculated using the created standard curve equations.

2.8. Statistical analysis

The quantitative analyses were performed three times and data was given as the mean ± standard deviation (±SD). To establish statistical significance, both the student's t-test and one-way analysis of variance (ANOVA) were utilized, with a $p < 0.05$ for significant differences.

3. RESULTS AND DISCUSSIONS

3.1. *Elsholtzia ciliata* extraction

To find the optimal EC extraction process, various conditions were surveyed, including (A) EtOH concentration, (B) temperature, (C) ratio of medicinal powder and EtOH, (D) extraction time, and (E) extraction time combined with ultrasound (**Figure 1**). Firstly, the greater the EtOH concentration, the lower the extracted polyphenol content (**Figure 1A**). This was due to the solvent polarity influences polyphenol solubility, and the polyphenol solubility has a direct impact on chemical recovery efficiency[28]. As a result, the ideal solvent concentration for the extraction method was determined to be EtOH 70%, with the highest polyphenol content.

Secondly, according to studies on the kinetics of biological component extraction, increasing the extraction temperature improves the efficiency of the process. When heated, the cell walls are shattered, therefore encouraging the transport of components into the extraction solvent[29]. Furthermore, when the temperature rises, the release of phenolic compounds increases owing to the hydrolysis of ester or ether linkages[30]. As a result, in this study, when the studied temperature was gradually increased from 40°C to 50°C, the recovered polyphenol content rose proportionally (**Figure 1B**). However, when the temperature further rises to 60°C, the polyphenol concentration falls. This may be explained by the fact that when the temperature rises, certain heat-sensitive and heat-lable biological molecules disintegrate, lowering the overall polyphenol concentration of the extract. As a result, the ideal temperature for this extraction procedure is 50°C.

In terms of the ratio of medicinal powder to solvent, as the amount of solvent increased from 1:10 to 1:40, the polyphenol content of the extract increased; however, as the ratio approached 1:45 and 1:50, the polyphenol content decreased (**Figure 1C**). As the amount of solvent increases, so does the capacity to wet the medicinal powder, to improve the solubility of polyphenol compounds, and to enhance the mass transfer process caused by the difference in concentration of the solid and liquid phases[31]. It is preferable to gradually raise the polyphenol content. However, after the amount of polyphenols extracted from medicinal plants has been maximized, increasing the volume of extraction solvent will diminish the polyphenol content of the extract. Therefore, the ratio of 1:40 was adopted for further experiments.

Regarding the extraction time, increasing the extraction time had little effect on the polyphenol concentrations (**Figure 1D**). Specifically, when the duration rose from 1 h to 2 h, the polyphenol content significantly increased from 9.36 to 9.77 mg GAE/g DPW, but as the period grew from 2 h to 5 h, the extracted polyphenol content remained constant. When employing the maceration method with a certain amount of solvent, the solute only dissolves into the solvent to a saturation level, thus, the polyphenol content was almost saturated and unaltered after 2 h of extraction. As a result, the optimal extraction time was 2 h.

Furthermore, employing ultrasonic energy to promote the diffusion process can reduce the extraction time while retaining the required material content. Specifically, when ultrasonic waves were combined, the polyphenol content peaked within the first 30 min (**Figure 1E**). Extended usage of ultrasound waves reduces polyphenol concentrations because ultrasound waves can create heat, which alters the structure of polyphenol molecules[32].

Conclusively, the ideal extraction conditions for EC included EtOH 70% as extracting solvent, a medicinal powder:solvent ratio of 1:40, a temperature of 50°C, an extraction time of 30 min, and with the application of ultrasonic waves. Utilizing this condition, the EC was extracted with 60 g plant powder for three extraction times and solvent evaporated, which possessed a moisture of 8.83±0.07%, an extraction efficiency (H%) of 5.375%, and a total polyphenol content of 93.45 mg GAE/g DPW. This result was in accordance with the previous study, as Pudziuvelyte *et al* reported phenolic levels ranging from 61.25±1.91 to 94.67±1.91 mg GAE/g DPW in the EC extracts, including leaves, stems, and flowers[26].

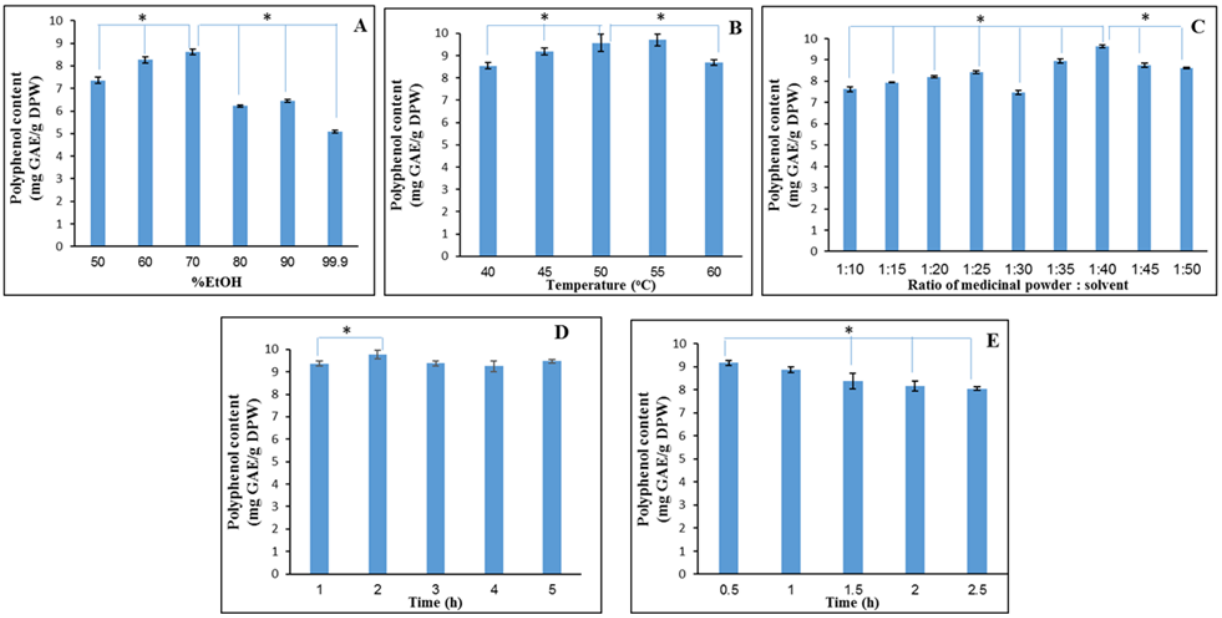

Figure 1. Polyphenol content in the EC under the survey conditions of (A) EtOH concentration, (B) temperature, (C) ratio of medicinal powder and EtOH, (D) extraction time, and (E) extraction time combined with ultrasound.

3.2. Preparation of the blank silk fibroin microparticles

The formulations of FMP have been well documented in previous publications [18,19]. Nevertheless, the effect of the desolvation solvent (i.e., EtOH) on the FMP size has not been thoroughly explored. To that end, this study first investigated the optimal fibroin/EtOH ratio to achieve the smallest size. For this, the particle sizes reduced as the amount of EtOH increased, achieving its lowest size at a 1:3 ratio (0.716 µm) and then progressively increases from 1:4 to 1:6 ratio (from 0.812 µm to 2.634 µm) (**Table 1**). When ethanol is added to a solution containing fibroin, the fibroin α-helical structure forms hydrogen bonds that change to the anti-parallel β-sheet structure, resulting in microparticles formation[19]. When the quantity of ethanol increases, the bond formation process accelerates, restricting the contact of the fibroin chains themselves, resulting in a smaller particle size. However, when the fibroin/EtOH ratio increased to ≥ 1:4, the particle formation process was significantly enhanced, thus, the particle density in the solution rose, and since the formulation duration was extended to 24 h, the particles could interact with one another to form clusters, consequently increased the hydrodynamic sizes. As a result, the fibroin/EtOH ratio of 1:3 was selected for the preparation of FMP-EC.

Table 1. Particle sizes of the blank FMP at various fibroin/EtOH ratios.

Fibroin/EtOH ratio	Size (µm)
1:1	5.7±2.5
1:2	1.2±0.6
1:3	0.7±0.1
1:4	0.8±0.2
1:5	2.6±1.4
1:6	2.6±2.1

3.3. FMP-EC particles characterizations

Two FMP-EC formula were prepared, the FMP-EC6 and FMP-EC9, with an initial polyphenol content of 1800 µg and 2700 µg, respectively. The FMP-EC6 possessed an average size of 0.7±0.1 µm, similar to that of the blank FMP, whereas the FMP-EC9 showed a bigger size of 3.2±0.2 µm. To explain this phenomenon, the formation of FMP-EC plays a role. The addition of EC ethanolic extract could induce the hydrophilic and hydrophobic chains of the fibroin molecules to be positioned alternatively, allowing the

fibroin molecules to form particles by the self-assembly process[5,23]. During this process, the polyphenol contents of the EC interacted with the fibroin via chemical bonding (i.e., hydrogen bonding, van der Waals forces, π-π interactions between benzene rings, and hydrophobic interactions between fibroin hydrophobic segments and polyphenols side chains), and thus, being encapsulated in the particle structures (**Figure 2**). As a result, when the initial polyphenol concentration is high, the amount of polyphenols loaded into the particles and adhered to its surface is also high, thus increasing the particle size. Additionally, the FMP-EC6 and FMP-EC9 showed similar loading efficiency of 29.91±1.54% and 31.69±0.97%, respectively, suggesting the saturation of the FMP in interacting with the EC polyphenol contents[33].

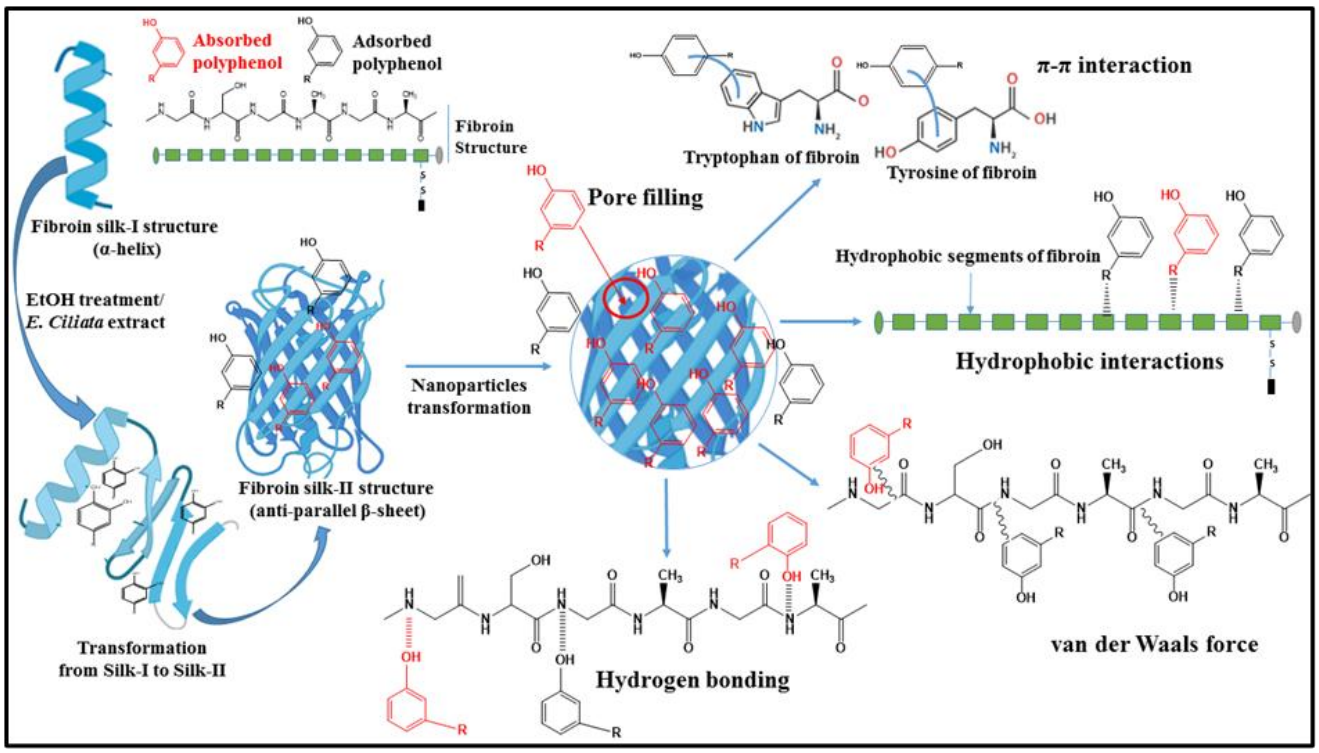

Figure 2. Mechanisms of the interactions of EC polyphenol and FMP.

In terms of the chemical interactions, the FT-IR spectra of the fibroin sample exhibits typical fibroin signals, such as amide I and amide II peaks at 1650-1500 cm^{-1} of C=O and N-H bonds, and amide III at 1240 cm^{-1} of C-N bonds (**Figure 3**), confirming the effective extraction of fibroin from silk cocoons[19]. Moreover, the blank FMP and FMP-EC show distinctive fibroin peaks comparable to fibroin, indicating the formulation process did not significantly alter the fibroin structures[18]. It is worth to notice that the amide I, II, and III peaks locations slightly shifted in the FMP-EC, which were due to the conformational changes from silk I (mainly α-helix structure) to silk II (mainly β-sheet structure) in the particle as a result of the addition of EC ethanolic extract. In addition to the normal peaks of the fibroin, the FMP-EC system exhibits additional peaks associated with polyphenol functional groups. Specifically, the region of 3000-3500 cm^{-1} is the hydrogen bond and -OH bond in the extract's alcoholic and phenolic components. This location also corresponds to the elongation bond of the -OH group in residual water formed after freeze-drying. The bond at 2800-2900 cm^{-1} is the C-H bond of the $-CH_2$ or C-H groups[34]. The peaks at 1019-1148 cm^{-1} represents C-O stretching and C-H bending bonds. These features were thoroughly proven in samples FMP-EC6 and FMP-EC9, indicating that the polyphenol-containing extract was successfully loaded into FMP. Furthermore, the crystallinity of FMP and FMP-EC was not statistically differed, suggesting the EC loading did not alter the particles inherent characteristics.

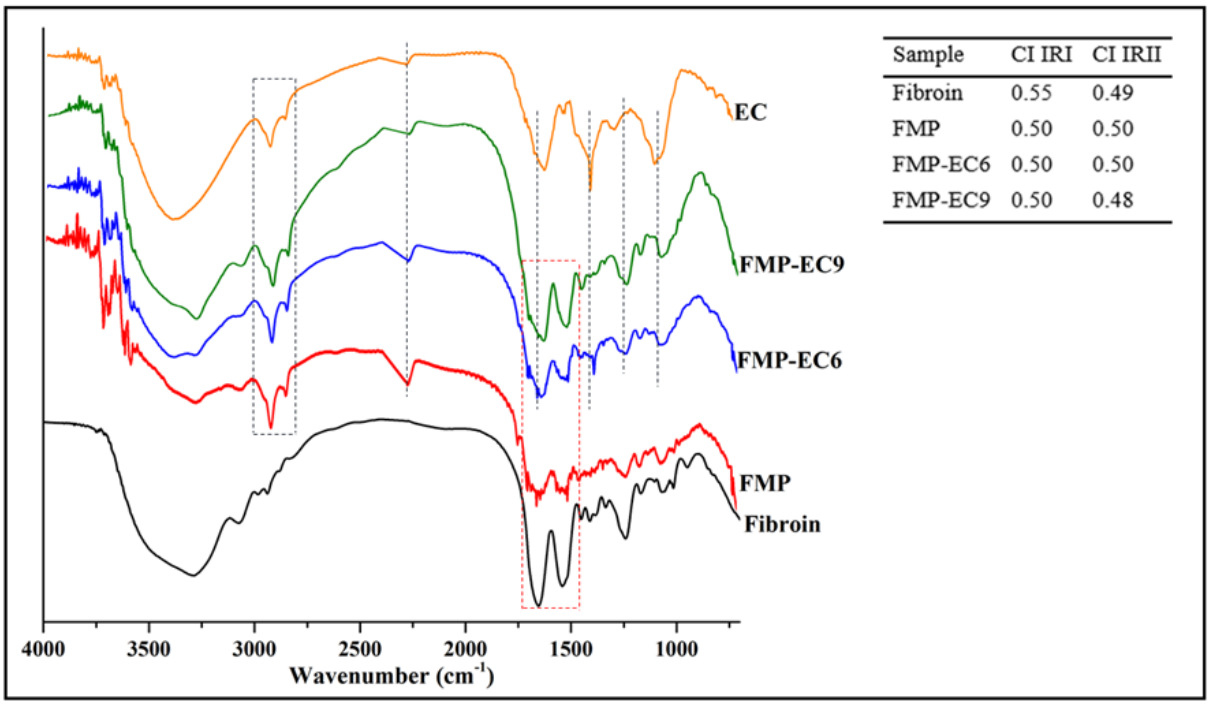

Sample	CI IRI	CI IRII
Fibroin	0.55	0.49
FMP	0.50	0.50
FMP-EC6	0.50	0.50
FMP-EC9	0.50	0.48

Figure 3. FT-IR spectra of fibroin, FMP, free EC, and FMP-EC, together with the sample crystallinity index.

Regarding the SEM images, the blank FMP particles before loading the EC was spherical with a smooth surface and aggregated pattern **(Figure 4A)**, in agreement with previous work[5,23]. The aggregated pattern was due to the inter-molecular interactions between the fibroin molecules[19]. Interestingly, when being loaded with the EC, both the FMP-EC6 and FMP -EC9 preserved its spherical form, while reduced the aggregated issue of the blank FMP **(Figure 4B and 4C)**. The reason for this is that polyphenols, when interacted with fibroin, may create additional forces between fibroin and polyphenols, as well as between polyphenols themselves, consequently solidified the particles, making them more compact. Moreover, these forces interrupt the fibroin-fibroin inter-molecular interactions, therefore, the particles aggregation was decreased.

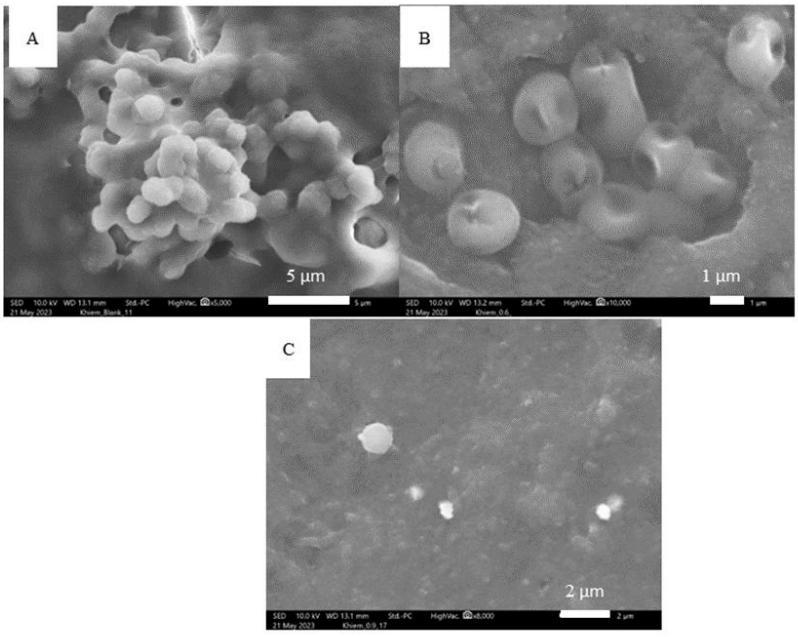

Figure 4. SEM images of the blank FMP (A), FMP-EC6 (B), and FMP-EC9 (C).

3.4. *In vitro* release profile in simulated skin condition

Figure 5 displays the polyphenol release process of FMP-EC6 and FMP-EC9, in simulated skin condition. Overall, the released polyphenol increased linearly over time, with the first burst-release initial phase at 30 min (30-40% polyphenol was released) and the second gradual-release phase for the remaining duration until 6 h, reaching 74.04% for FMP-EC6 and 61.93% for FMP-EC9. During the entire release time, the amount of polyphenol was adequate to exert anti-oxidative activity, as the minimum release amount was almost two times higher than the IC_{50} of the particles (discussed in the next section). The initial rapid release could be due to the weakly bound water-soluble polyphenol compounds located on the particles surfaces, which dissolved favorably in the release medium. On the other hand, the gradual release phase was attributed to the strongly bound lipophilic polyphenol compounds that interacted with the fibroin molecules in the particle cores (**Figure 2**). This fact proved the research hypothesis on using FMP to control the release rate of polyphenol compounds in EC on the skin surfaces.

Notably, the release rate for FMP-EC6 was more rapid compared to FMP-EC9, which shows a more gradual release. The gap between the two formulations remains consistent throughout the time course. This was possibly due to the difference in particle sizes. The FMP-EC6 possessed a nano-size of 0.7±0.1 µm, whereas the FMP-EC9 showed a micron-size of 3.2±0.2 µm. Thus, the high surface-area-to-volume ratio of FMP-EC6 enhances their contact with the dissolution medium, consequently increasing the release rate[35].

Lastly, when fitted in different release model, the release process of both particles was congruent with some mathematical models, with R^2 of > 0.9 **(Table 2)**. For FMP-EC6, the three R^2 values from the First-order, Higuchi, and Korsmeyer-Peppas models were more than 0.9, indicating that the release process was identical to the processes in all three models. Furthermore, based on the beginning circumstances, the particles exhibited polymeric characteristics, and the matrix structure is compatible with the Korsmeyer-Peppas model. The number n = 0.6893 (0.45 < n < 0.9) indicates that the released particles followed a diffusion process with coupled decay[36], which aligns with the experimental release data. Similarly, the release profile of FMP-EC9 followed well with the diffusion process and decay of the fibroin matrix, with n = 0.6509[37]. Conclusively, the particles first rapidly released the water-soluble EC polyphenols on the surfaces, then, the lipophilic EC polyphenols on the core was gradually diffused out due to the slow degradation of fibroin matrix in the medium.

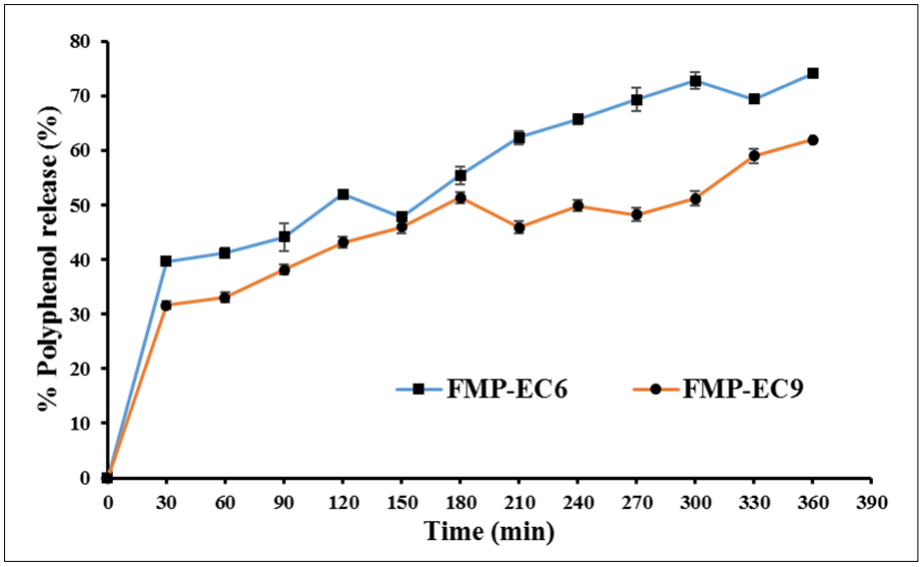

Figure 5. Polyphenol release profile in simulated skin condition of FMP-EC6 and FMP-EC9.

Table 2. The R^2 value of different release kinetic model of the FMP-EC.

Sample	Zero-order	First-order	Higuchi	Hixson-Crowell	Korsmeyer-Peppas
FMP-EC6	0.7926	0.9174	0.9376	0.8864	0.9135
FMP-EC9	0.7278	0.8229	0.9019	0.7961	0.9097

3.5. Antioxidant activity test

The antioxidant activity of EC, FMP-EC6, and FMP-EC9 was assessed using the DPPH free radical scavenging activity **(Table 3)**. Firstly, the free EC had lesser antioxidant activity than vitamin C, yet it still falls within the category of potent/very-active antioxidants[38]. Comparing to the EC IC_{50} of a previous work, which demonstrated a value of 495.80±17.16 µg/mL[17], the extract in this study exhibited superior activity with an IC_{50} of 12.87±0.82 µg/mL, indicating the effect of geography on the plant potency. Secondly, the FMP-EC showed weaker antioxidant activity than the free EC, which possibly due to the slow release of polyphenols from the particles. Since the incubation time of the DPPH assay was only 30 min, with limited solvent, the released polyphenol amount from the particles was < 30%. Nevertheless, even at this low release rate, the total amount of EC polyphenol was adequate for the antioxidant activity. Moreover, the particles could also prolong and sustain the polyphenol release for 6 h, which benefits the long-term use of this product for skin cosmetic.

Table 3. IC50 values of DPPH anti-oxidative activity of vitamin C, free EC, and FMP-EC.

Sample	Linear equation	IC_{50} (µg/mL)
Vitamin C	$y = 11.311x – 0.5019$ ($R^2 = 0.9954$)	4.46±0.04
Free EC	$y = 3.98x – 1.2054$ ($R^2 = 0.9981$)	12.87±0.82
FMP-EC6	$y = 0.231x + 6.0087$ ($R^2 = 0.9596$)	190.44±2.31
FMP-EC9	$y = 0.3119x – 0.0677$ ($R^2 = 0.9574$)	160.52±1.98

4. CONCLUSIONS

The study effectively extracted EC, encapsulated the extract in FMP, physicochemical characterized the particles, and determined their release profile and antioxidant activity, for the purpose of anti-oxidative skin cosmetic. The particles were successfully produced by one-pot desolvation process with appropriate properties, sustain release the EC polyphenol for 6 h in an environment that mimics the skin pH, with a release efficiency of more than 70%, following Korsmeyer-Peppas model, and preserve the EC antioxidant activity. In conclusions, the study demonstrates the potential use of the FMP-EC as a skin cosmetic, and the particles could be further investigated to be a commercial product.

5. ACKNOWLEDGEMENTS

The authors acknowledge Can Tho University, Can Tho University of Medicine and Pharmacy, and Dong Nai Technology University for supporting this research.

Conflict of interest
None to declare.

Funding
None to declare.

Article info:
Received July 13, 2024
Received in revised August 23, 2024
Accepted October 4, 2024

REFERENCES

1. Clarke LH, Korotchenko A. Aging and the Body: A Review. Can J Aging 2011;30(3):495–510; doi: 10.1017/S0714980811000274.
2. Walker M. Human skin through the ages. International Journal of Pharmaceutics 2022;622:121850; doi: 10.1016/j.ijpharm.2022.121850.
3. Karimkhani C, Dellavalle RP, Coffeng LE, Flohr C, Hay RJ, Langan SM, et al. Global Skin Disease Morbidity and Mortality. JAMA Dermatol 2017;153(5):406–12; doi: 10.1001/jamadermatol.2016.5538.
4. Zhang S, Duan E. Fighting against Skin Aging. Cell Transplant 2018;27(5):729–38; doi: 10.1177/0963689717725755.
5. Pham DT, Huynh QC, Lieu R, Nguyen VB, Tran VD, Thuy BTP, et al. Controlled-Release Wedelia trilobata L. Flower Extract Loaded Fibroin Microparticles as Potential Anti-Aging Preparations for Cosmetic Trade Commercialization. Clinical, Cosmetic and Investigational Dermatology 2023;16:1109–21; doi: 10.2147/CCID.S405464.
6. Martelli G, Giacomini D. Antibacterial and antioxidant activities for natural and synthetic dual-active compounds. European Journal of Medicinal Chemistry 2018;158:91–105.
7. Zagoskina NV, Zubova MY, Nechaeva TL, Kazantseva VV, Goncharuk EA, Katanskaya VM, et al. Polyphenols in Plants: Structure, Biosynthesis, Abiotic Stress Regulation, and Practical Applications (Review). Int J Mol Sci 2023;24(18):13874; doi: 10.3390/ijms241813874.
8. Ganesan K, Xu B. A Critical Review on Polyphenols and Health Benefits of Black Soybeans. Nutrients 2017;9(5); doi: 10.3390/nu9050455.
9. Omodanisi EI, Aboua YG, Oguntibeju OO. Assessment of the Anti-Hyperglycaemic, Anti-Inflammatory and Antioxidant Activities of the Methanol Extract of Moringa Oleifera in Diabetes-Induced Nephrotoxic Male Wistar Rats. Molecules 2017;22(4); doi: 10.3390/molecules22040439.
10. Odongo GA, Schlotz N, Herz C, Hanschen FS, Baldermann S, Neugart S, et al. The role of plant processing for the cancer preventive potential of Ethiopian kale (Brassica carinata). Food & Nutrition Research ISSN: 2017;61.
11. Sajid M, Khan MR, Shah SA. Investigations on anti-inflammatory and analgesic activities of Alnus nitida Spach (Endl). stem bark in Sprague Dawley rats Moniba. Journal of Ethnopharmacology 2017;198:407–16.

12. Reboredo-Rodríguez P, Figueiredo-González M, González-Barreiro C. State of the Art on Functional Virgin Olive Oils Enriched with Bioactive Compounds and Their Properties. International Journal od Molecular Sciences 2017;18:668.
13. Léotoing L, Wauquier F, Davicco M-J. The phenolic acids of Agen prunes (dried plums) or Agen prune juice concentrates do not account for the protective action on bone in a rat model of postmenopausal osteoporosis. Nutrition Research 2016;36:161–73.
14. Meng ZQ, Li JL. Antioxidant and Angiotensin-Converting Enzyme Inhibitory Activity of Eucalyptus camaldulensis and Litsea glaucescens Infusions Fermented with Kombucha Consortium Claudia. Food Technol Biotechnol 2011;54(6):367–74.
15. Miyamoto T, Zhang X, Ueyama Y, Apisada K, Nakayama M, Suzuki Y, et al. Development of Novel Monoclonal Antibodies Directed against Catechins for Investigation of Antibacterial Mechanism of Catechins. Journal of Microbiological Methods 2017;137:6–13; doi: 10.1016/j.mimet.2017.03.014.
16. Huynh DTM, Le M-NT, Tran VD, Tran V-H, Pham DT. Native Medicinal Plants (Moringa oleifera Lam, Brucea javanica (L.) Merr., Eclipta prostrata (L.), Callisia fragrans (Lindl.) Woodson, and Zingiber zerumbet (L.) Smith) in An Giang, Vietnam: A Preliminary Investigation for Rhabdomyosarcoma Treatments using in-vitro RD cell cytotoxicity test. Jordan Journal of Pharmaceutical Sciences 2023;16(4):830–41; doi: 10.35516/jjps.v16i4.1365.
17. Phong HX, Viet NT, Quyen NTN. Phytochemical screening, total phenolic, flavonoid contents, and antioxidant activities of four spices commonly used in Vietnamese traditional medicine. Materials Today: Proceedings journal 2022;56:A1–A5.
18. Nguyen NY, Nguyen TNP, Huyen NN, Tran VD, Quyen TTB, Luong HVT, et al. Onto the differences in formulating micro-/nanoparticulate drug delivery system from Thai silk and Vietnamese silk: A critical comparison. Heliyon 2023;9(6):e16966; doi: 10.1016/j.heliyon.2023.e16966.
19. Pham DT, Nuttawut S, Tiyaboonchai W. Crosslinked fibroin nanoparticles using EDC or PEI for drug delivery: physicochemical properties, crystallinity and structure. J Mater Sci 2018;53:14087–103.
20. Pham DT, Nguyen TL, Nguyen TTL, Nguyen TTP, Ho TK, Nguyen NY, et al. Polyethylenimine-functionalized fibroin nanoparticles as a potential oral delivery system for BCS class-IV drugs, a case study of furosemide. Journal of Materials Science 2020; doi: 10.1007/s10853-023-08640-y.
21. Pham DT, Ha TKQ, Nguyen MQ, Tran VD, Nguyen VB, Quyen TTB. Silk fibroin nanoparticles as a versatile oral delivery system for drugs of different biopharmaceutics classification system (BCS) classes: A comprehensive comparison. Journal of Materials Research 2022;37(23):4169–81; doi: 10.1557/S43578-022-00782-0.
22. Konishi T, Kurokawa M. The Structure of Silk Fibroin-α. Sen'i Gakkaishi 1968;24(12):550–554; doi: 10.2115/fiber.24.550.
23. Pham DT, Nguyen DXT, Lieu R, Huynh QC, Nguyen NY, Quyen TTB, et al. Silk nanoparticles for the protection and delivery of guava leaf (Psidium guajava L.) extract for cosmetic industry, a new approach for an old herb. Drug Delivery 2023;30(1):2168793; doi: 10.1080/10717544.2023.2168793.
24. Paladines-Quezada D, Cueva C, Gil-Muñoz R, Cenis JL, Bartolomé B, Moreno-Arribas MV, et al. Preparation, characterization and gastrointestinal stability of silk fibroin nanoparticles loaded with red wine polyphenols. Food Bioscience 2023;52:102431; doi: 10.1016/j.fbio.2023.102431.
25. Pham DT, Tiyaboonchai W. Fibroin-coated poly(ethylenimine)-docusate nanoparticles as a novel drug delivery system. Current Science 2021;121(6):775–780;doi:10.18520/CS/V121/I6/775-780.
26. Singleton VL, Orthofer R, Lamuela-Raventós RM. [14] Analysis of total phenols and other oxidation substrates and antioxidants by means of folin-ciocalteu reagent. Methods in Enzymology 1999;299:152-78.
27. Bierman W. The temperature of the skin surface. Journal of the American Medical Association 1936;106(14):1158–1162; doi: 10.1001/jama.1936.02770140020007.
28. Herrera-Pool E, Ramos-Díaz AL, Lizardi-Jiménez MA, Pech-Cohuo S, Ayora-Talavera T, Cuevas-Bernardino JC, et al. Effect of solvent polarity on the Ultrasound Assisted extraction and antioxidant activity of phenolic compounds from habanero pepper leaves (Capsicum chinense) and its identification by UPLC-PDA-ESI-MS/MS. Ultrasonics Sonochemistry 2021;76:105658; doi: 10.1016/j.ultsonch.2021.105658.
29. Boateng J, Verghese M, Walker LT, Ogutu S. Effect of processing on antioxidant contents in selected dry beans (Phaseolus spp. L.). LWT - Food Science and Technology 2008;41(9):1541–1547; doi: 10.1016/j.lwt.2007.11.025.
30. Cacace JE, Mazza G. Mass transfer process during extraction of phenolic compounds from milled berries. Journal of Food Engineering 2003;59(4):379–389; doi: 10.1016/S0260-8774(02)00497-1.
31. Qu W, Pan Z, Ma H. Extraction modeling and activities of antioxidants from pomegranate marc. Journal of Food Engineering 2010;99(1):16–23; doi: 10.1016/j.jfoodeng.2010.01.020.
32. Pudziuvelyte L, Jakštas V, Ivanauskas L, Laukevičienė A, Ibe CFD, Kursvietiene L, et al. Different extraction methods for phenolic and volatile compounds recovery from Elsholtzia ciliata fresh and dried herbal materials. Industrial Crops and Products 2018;120:286–294; doi: 10.1016/j.indcrop.2018.04.069.
33. Pham DT, Saelim N, Tiyaboonchai W. Paclitaxel loaded EDC-crosslinked fibroin nanoparticles: a potential approach for colon cancer treatment. Drug Delivery and Translational Research 2019; doi: 10.1007/s13346-019-00682-7.
34. Sivam AS, Sun-Waterhouse D, Perera CO, Waterhouse GIN. Application of FT-IR and Raman spectroscopy for the study of biopolymers in breads fortified with fibre and polyphenols. Food Research International journal 2011;50(2):574–585.
35. Navya PN, Daima HK. Rational engineering of physicochemical properties of nanomaterials for biomedical applications with nanotoxicological perspectives. Nano Converg 2016;3:1; doi: 10.1186/s40580-016-0064-z.
36. Brannon-Peppas L, Peppas NA. The Equilibrium Swelling Behavior of Porous and Non-Porous Hydrogels. 1990;8:67–102; doi: 10.1016/B978-0-444-88654-5.50009-1.
37. Ding Y, Dou C, Chang S, Xie Z, Yu D-G, Liu Y, et al. Core–Shell Eudragit S100 Nanofibers Prepared via Triaxial Electrospinning to Provide a Colon-Targeted Extended Drug Release. Polymers 2020;12:1–13.
38. Fatmawaty, Anggreni NGM, Fadhil N, Prasasty VD. Potential In Vitro and In Vivo Antioxidant Activities from Piper Crocatum and Persea Americana Leaf Extracts. Biomedical and Pharmacology Journal 2019;12(2):661–667.